Vibration Bearing Diagnostic System Machine Learning

S. Sinutin, S. Lebedev, E. Sinutin

***Abstract*: The article shows the possibility of using a mathematical model of a bearing with various types of defects for machine learning of the vibration diagnostic system. A plane geometric model of a radial bearing with two degree of freedom is considered in detail, a system of differential equations describing the nature of the motion of moving masses in the mechanical bearing system is presented. A formula is obtained for calculating the total kinematic disturbance, the calculation of which is associated with significant computational costs. The article proposes an alternative calculation method, namely, modeling the profile of kinematic disturbances in the time domain, which will minimize computational costs. The adequacy of the proposed method is confirmed by calculations in Matlab and comparison with experimental data.**

The development of equipment maintenance systems for the actual technical condition is relevant as in the case of operation of facilities of increased danger Gerike, and in the case of the operation of expensive equipment Pisarev and Vaganov, where the diagnosis with disassembling the machine leads to large financial losses. Diagnostics of equipment by vibration parameters allows fixing defects in the early stages during normal operation without the need to disassemble the units and take them out of service.

***Keywords*: Acceleration spectrum, bearing, machine learning, neural network, rolling element defects, vibration velocity.**

I. INTRODUCTION

Currently, the most popular analysis methods are threshold methods (for example, for turbines this is an excess of the threshold value of the mean square value (MSV) of the vibration velocity or rotor displacement value) and spectral methods. The second ones mainly rely on Fourier analysis and observation of certain parts of the spectrum. An increase in the power of the signal spectrum in these areas signals a developing defect. Due to the nonlinear nature of defects, an expert who is able to differentiate artifact records and real manifestations of defects is required for a qualitative assessment of processed signals [1, 2].

To automate this process, you can use machine learning methods, in particular neural networks for time series analysis. Rozhkov and Shadsky [3] refer to 4 main diagnostic methods:

- according to the MSV of vibration velocity;
- the spectra of vibration signals;
- the ratio of peak/background vibration signal;
- the spectrum of the envelope of the vibration signal.

An analysis of spectrum of the envelope of a vibration signal is proposed as the most effective method. The usage of a previously taught neural network on the unique vibration patterns of malfunctions is proposed to recognize a rotor unit malfunction. It should be noted that the implementation of such diagnostic methods requires large amounts of data for training the neural network, especially when it comes to classification problems. All of this lead either to an excessive complication of the structure of the neural network (which in turn leads to the effect of "memory" - the neural network simply remembers the data of the training sample, but does not generalize it), or to the rejection of neural network modeling. Suggested solutions to the problem include:

- reduction in volume or rejection of the test sample;
- pseudo-random generation of new examples;
- structural changes in the neural network or neural network model.

To solve the problem of vibration diagnostics, you can turn to the second one option, complicating the method of generating new examples. The main structures of neural networks are the multilayer perceptron [5], and deep belief networks (DBN) [6]. The sample size in the first case was 2500 samples of MSV vibration velocity, in the second case, the implementation of vibration signals was used, in the amount of 64 for each defective and normal condition of the bearing.

II. METHODOLOGY

The problem of small training samples can be solved by constructing a mathematical model of the bearing, with the possibility of introducing "defects". Using this model, one can generate signals and supplement the training sample unlike bootstrap methods and should not be afraid of saturation due to the lack of really new data [4].

For the effective application of neural network modeling, it will be necessary to use not only signals with isolated defects, but also variants of complex faults. Otherwise, the neural network may be not able to cope with the problem of classifying faults (the problem of giving an answer "I don't know" or "both" [7]). This is easy to implement by using the mathematical model of the bearing. In a real bearing, it is a difficult engineering task to simultaneously introduce several defects into the structure.

The problem of "ideality" of the training sample data should be noted. If the neural network is trained on idealized model data, real signals taken from the bearings of the bearings may be too noisy for it.

Revised Manuscript Received on November 05, 2019.

***** Correspondence Author

Sergey Sinutin, Institute of Radio Engineering Systems and Control, Southern Federal University. Email: sasinyutin@sfedu.ru

Sergey Lebedev*, Design Center "Design of integrate microelectronic system", National Research University of Electronic Technology (MIET), Moscow, Russian Federation. Email: lebedevsergey11@rambler.ru

Evgeniy Sinutin, Scientific and Technical Center "Technocentre" of Southern Federal University. Email: dark_elf4@mail.ru

In addition, when developing a model, the presence of tolerances in the structural elements of bearings should be taken into account.

In this work, we used a method for modeling the profile of the kinematic disturbance in the time domain, which consists in representing the kinematic disturbance A_i as a program function with argument *t* (current simulated time), from which the instantaneous phase ψ is obtained, and then the defect is modeled as a deterministic function ψ. Then the additive noise of random surface defects is added.

This method will significantly reduce computational costs with the machine learning method of the vibration diagnostics system.

III. RESULTS

The initial bearing model is a flat geometric model of a radial bearing with two degree of freedom in radial directions [11, 12]. Gasparov gives a bearing model in the form of a mechanical system with a combination of linear and nonlinear stiffnesses [8-10]. Bearing elements are considered as rigid bodies locally deformable in small contact areas. In this case, the bearing assembly is represented as a system of interconnected concentrated masses. The oscillations of the elements of the rotor assembly will be determined by the vector sum of their movements along the directions of their contact with the rolling bodies. In Fig. 1, the geometric model (a) and the generalized calculation scheme (b) of the rotor support are shown. The model has one fixed and several movable coordinate systems rigidly connected with balls in the cage. Moving coordinate systems rotate relatively motionless with an angular velocity equal to the speed of rotation of the separator ω_c, i.e. the geometric center of the ball lies on the axis of the corresponding moving coordinate system.

The following assumptions are made in the model:

- there is no sliding of balls,
- the treadmill profile is unchanged,
- the contact angle is constant,
- there is no gyroscopic effect when spinning balls.

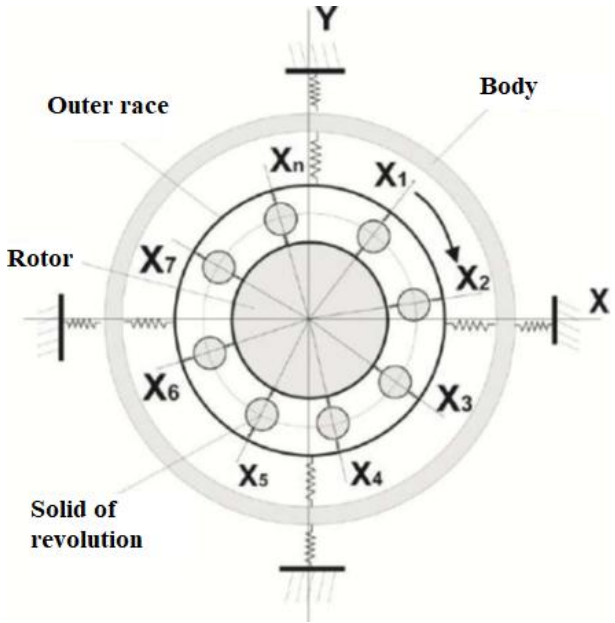

(a)

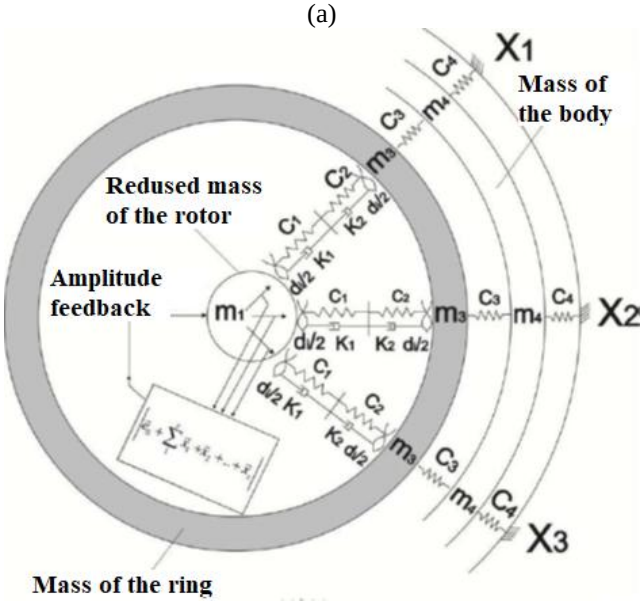

(b)

Fig. 1. The geometric model (a) and the design scheme (b) of the bearing support of the rotor assembly

The design scheme in Fig. 1 (b) takes into account the influence of amplitude feedback, i.e. the effect of rotor movement on the amplitude of the periodic disturbing force caused by the initial rotor imbalance.

Periodic force will be calculated by the formula:

$$F = m_1 e \omega_p \quad (1)$$

where m_1 is the rotor mass brought to the support, e is the dynamic eccentricity, ω_p is the angular velocity of the rotor.

Denoting the oscillations of the cased mass of the housing m_4 supported along the *n-th* movable axis as x_4 for their projections relative to the *Y* axis of the fixed coordinate system, we can write:

$$(x_{4_n})_Y = x_{4_n} \cos(\omega_c t + \phi_0 + \frac{2\pi(n-1)}{z}) \quad (2)$$

where x_{4n} is the oscillation of the m_4 mass along the *n-th* moving axis, and the expression under the cosine sign is the angle between the moving axis x_n and the *Y* axis of the fixed coordinate system.

Then, from geometric considerations, the resulting displacement of the $m_4$mass along the *Y* axis will be equal to the sum of the projections of the oscillations along the moving axis onto the fixed axis:

$$x_{4_Y} = \sum_n^z 1(x_{4_n})_Y \quad (3)$$

where z is the number of rolling elements in the bearing.

The stiffness characteristics of rolling bearings, especially ball bearings, have a pronounced nonlinear character. Installing a rolling bearing in a support with linear stiffness c_3 of the "outer ring-node" subsystem (Fig. 2) creates a constructive mechanical system with a combination of linear and nonlinear stiffnesses, where:

- m_1 is the rotor mass brought to the support;
- m_2 is the mass of the ball;
- m_3 is the mass of the outer ring;

- m_4 is the mass of the rotor assembly body reduced to the support;
- c_1 is the nonlinear rigidity of the subsystem "inner ring-ball";
- k_1 is the coefficient of viscous resistance of the subsystem "inner ring-ball";
- c_2 is the nonlinear rigidity of the subsystem "ball-outer ring";
- k_2 is the coefficient of viscous resistance of the subsystem "ball-outer ring";
- c_3 is the rigidity of the "outer ring-node" subsystem;
- c_4 is the rigidity of the "node-bed" subsystem;
- $F_{in.ten.}$ is the force preload (initial tension);
- F_{rotor} is the periodic force caused by an imbalance of the rotor;
- $F_{cut.force}$ is cutting force reduced to the support;
- d_i is the error profile of the ball, expressed as a change in its diameter;
- $F_{centr.ball}$ is centrifugal force of the ball, the value of which increases with the speed of the separator;
- k_3, k_4 are the coefficients of viscous deformation resistance of the subsystems "outer ring-node" and "node-bed", respectively.

These coefficients (k_3 and k_4) cannot be taken into account in view of the smallness of their values. Let's consider an oscillatory system along 1 of the moving axes. Such an oscillatory system consists of 4 elastically and dissipative connected concentrated masses (Fig. 2, a).

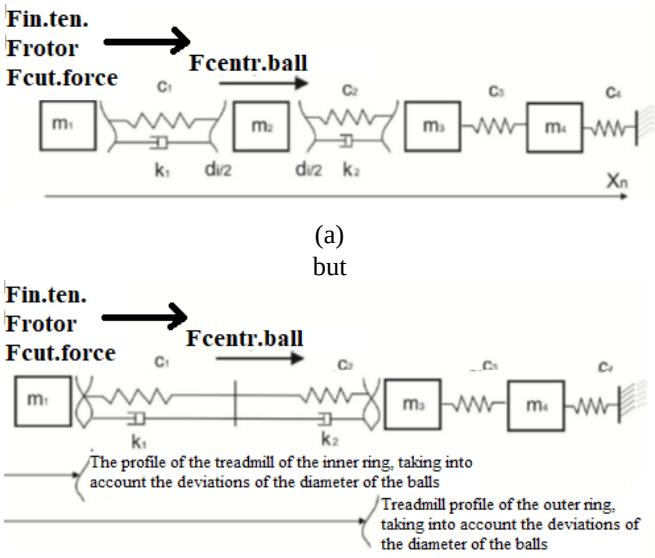

Fig. 2. A mechanical system along one of the movable axes, taking into account (a) and without taking into account (b) the mass of the ball

We neglect the mass of the ball m_2 and take it equal to 0 due to the fact that the mass of the ball is less than the masses of the other elements by more than an order of magnitude and thus simplify the mechanical system to a system of 3 concentrated masses (Fig. 2, b). The centrifugal force acting on the ball can also be neglected accordingly. In this case, the influence of the error in the profile of the ball is preserved. The system of differential equations that describe the motion of the simplified mechanical system masses shown in Fig. 2 is given below:

$$\begin{cases} m_1 \ddot{x}_1 = F_{source} - c_{gen}[x_1 - x_3 + A(t)] - k_{gen}[\dot{x}_1 - \dot{x}_3 + \dot{A}(t)] \\ m_3 \ddot{x}_3 = c_{gen}[x_1 - x_3 + A(t)] + k_{gen}[\dot{x}_1 - \dot{x}_3 + \dot{A}(t)] - c_3(x_3 - x_4) \\ m_4 \ddot{x}_4 = -c_4 x_4 + c_3(x_3 - x_4) \end{cases} \quad (4)$$

where c_{gen} is the total nonlinear rigidity of the rotor-outer ring subsystem, $A(t)$ is the total kinematic perturbation caused by irregularities in the racetrack profiles of the rings and the ball, k_{gen} is the total viscous drag coefficient equal to the sum of the coefficients k_1 and k_2, x_i is the displacement corresponding to *i-th* of the same mass, Source - the projection of the vector of the total force impact from the rotor side to the given axis:

$$F_{source} = F_{in.ten.} + F_{period} + F_{grav.} + F_{cut.force} \quad (5)$$

where $F_{in.ten.}$ is the preload force, F_{period} is the periodic force caused by imbalance of the rotor, $F_{grav.}$ is the gravity, the value of which depends on the location of the rotor, $F_{cut.force}$ is the cutting force reduced to the support. Contact deformation is determined, based on the static elastic characteristic according to the Hertz theory, which considers the static contact of two bodies under the following assumptions:

- the materials of the contacting bodies are homogeneous, isotropic and perfectly elastic;
- the contact area is small compared with the radius of curvature of the surfaces;
- the pressure forces are normal to the contact surface of bodies;
- no friction.

Numerous studies of Leontiev [12, 13] pointed out that under static loading, the dimensions of the contact and proximity surfaces calculated by Hertz are in good agreement with the experimentally measured ones. The formula for deformation can be written in the form:

$$\delta = a \cdot F_3 \quad (6)$$

where a is a numerical coefficient depending on the size of the bearing and the elastic constants of the material of the rings and balls [14].

In the Table 1, the geometric characteristics of the angular contact ball bearing of the model 214 and the approximate data of the mass-stiffness characteristics of the model are shown.

Table 1. The geometric characteristics of the angular contact ball of the model 214

The characteristic	Value
The average diameter of the bearing, mm	125
Contact angle, °	15
Diameter of rolling bodies (balls), mm	17.462
Number of rolling bodies (balls), n	10
The radius of the grooves, mm	2
Damping in the bearing, Nsec/m	100-400
m_1 the reduced rotor mass, kg	1.21
m_4 the mass of the body, kg	3.0
m_3 the mass of the outer ring, kg	0.82
c_3 the rigidity of the subsystem "outer ring-node", N/m	$10^7 \div 2 \cdot 10^7$
c_4 the rigidity of the subsystem "node-bed", N/m	$10^8 \div 2 \cdot 10^8$

In further calculations, modeling, and plotting, the data in Table 1 will be used. Using the data of Table 1, the expression of contact deformation can be written in the form of formula (6):

$$\delta = 33.3 \cdot 10^{7} \cdot F^{3/2} \quad (6)$$

The quantity $A(t)$ given in formulas (4) is the total kinematic perturbation caused by the unevenness of the raceways of the rings and the rolling lines of the balls. Such disturbances can be caused both by manufacturing technological errors and by defects that have arisen at the operational stage. In the general case, the kinematic perturbation function can be approximated by any series, but the approximation by the trigonometric series is most often used. In this case, the profiles of racetracks are presented in the form of a Fourier series as a function of changing the radii, and the ball line of rolling as a function of changing the diameter of a given ball (Fig. 3), where $R_I(\psi)$ is the radius changing function that describes the profile of the race tracks of the inner ring, $R_O(\psi)$ is the radius change function that describes the treadmill profile of the outer ring, $D_B(\psi)$ is the function that describes the change in the diameter of the balls.

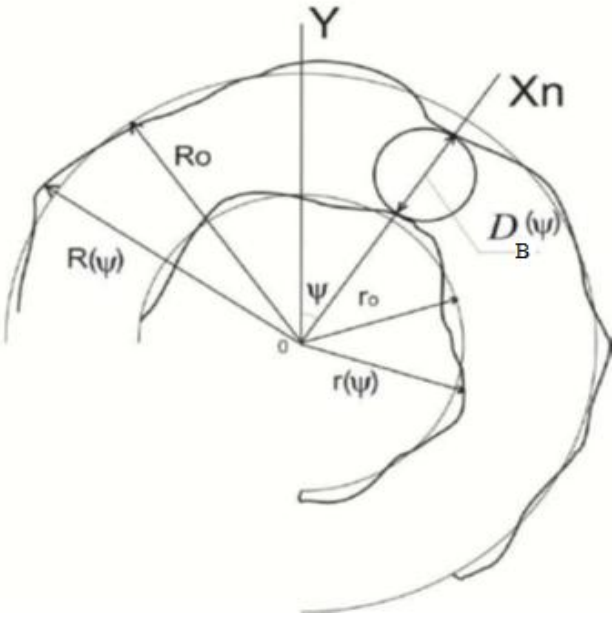

Fig. 3. Graphical explanation of the kinematic disturbance function

In view of the foregoing, the expression for the kinematic disturbance is written as:

$$A_i(t) = (R_O(\psi) - R_I(\psi) - D_{B_i}(\psi)) \quad (7)$$

where $R_O(\psi)$, $R_I(\psi)$, $D_{Bi}(\psi)$ are the radius of the treadmill profiles of the outer and inner rings of the bearing and the diameter of the *i-th* ball at the point of contact with the treadmills.

The parameters $R_O(\psi)$, $R_I(\psi)$, $D_{Bi}(\psi)$ are functions of the phase (ψ) (Fig. 3), which changes over time with angular velocities: separator ω_c, rotor relative to the separator (ω_p - ω_c), the 2nd ball spinning ω_B, respectively.

Under the condition of expansion in a Fourier series, formula (7) can be transformed into formula (8):

$$\begin{aligned} A_i(t) &= R_{O_0} - R_{I_0} - D_{B_0} + \\ &+ \sum_{n=1}^{\infty} A_n \cos(n\psi + \omega_c + \frac{2\pi}{z}(i-1) + \phi_n) - \\ &- \sum_{m=1}^{\infty} A_m \cos(m\psi + (\omega_p - \omega_c)t + \frac{2\pi}{z}(i-1) + \phi_m) - \\ &- \sum_{k=1}^{\infty} A_k \cos(k\psi + 2\omega_B t + \phi_k) \end{aligned} \quad (8)$$

where ω_p, ω_c, ω_B are the rotational speeds of the rotor, separator and spinning balls, respectively, i is the number of the ball, z is the number of balls in the bearing race, A_n, A_m, A_k are the amplitudes of the harmonic components the radius of the treadmill profiles of the outer and inner rings and the diameters of the balls, respectively, ϕ_n, ϕ_m , ϕ_k are the initial phases of the harmonic components of the radius of the treadmill profiles of the outer and inner rings and the diameters of the balls, respectively; R_{O0} , R_{I0} , D_{B0} are constant components of the radius of the treadmill profiles of the outer and inner rings and the diameter of the balls.

From the formula (8) it is clear that the solution of the system (4) will require significant computational costs at each integration step. For the normal reproduction of defects with sharp edges, about 10 members of the Fourier series are needed. For a 214 model bearing, the parameter *z=10*, therefore, even for a one-step integration method there will be 120 calculations of trigonometric functions at each step, for the Runge-Kutta method there will already be 480 calculations of trigonometric functions at each step, and with an adaptive choice of the step, such calculations will be even greater.

Taking into account the simulation of rotor acceleration, each training set should be at least 10 seconds of real time. For modeling 10 seconds of real time, 256,000 steps are required, therefore, for the one-step method, 30,720,000 calculations of trigonometric functions will be required, which is obviously completely unacceptable.

In this paper, a different approach was used, namely, modeling the profile of kinematic disturbances in the time domain. For this, formula (7) is represented by a program function with argument *t* (current simulated time), from which the instantaneous phase ψ is obtained, and then the defect is modeled as a deterministic function ψ, and the additive noise of random surface defects is added based on the following condition,

if Psi>=Psid and Psi<=Psi_d+Dd,

then R=R-H_d,

otherwise R=R_0+LPFd (Random (H_v)) - H_v/2),

where Psi is the current phase, Psi*d* is the defect onset phase, D_d is the defect duration (in radians), H_d is the defect depth, R_0 is the initial radius of the outer ring (inner ring, ball), LPF_d is a low-pass filter, forming a random profile of white noise, Random (H_v) - H_v/2 is a white noise generator with an amplitude of H_v and zero mean.

Such a method for determining the kinematic perturbation will require the use of the random and LPF functions only 12 times [25, 26].

The proposed model is the most complete, i.e. takes into account most of the factors affecting the dynamic quality of the support and the rotor assembly as a whole. The main differences between this model and others available in the literature are the consideration of

the nonlinear characteristics of the contact deformation of the support and relatively low computational costs [15, 16]. To solve the system of differential equations (4), the Matlab package was used, in particular, the Ode45 solver with a uniform constant integration step of 1/25600 sec. This approach was chosen because of a further mechanical experiment, carried out with a model 214 bearing, the vibration parameters of which were measured with a sampling frequency of 25600 Hz [17-20].

The simulation results are presented in Figures 4-9.

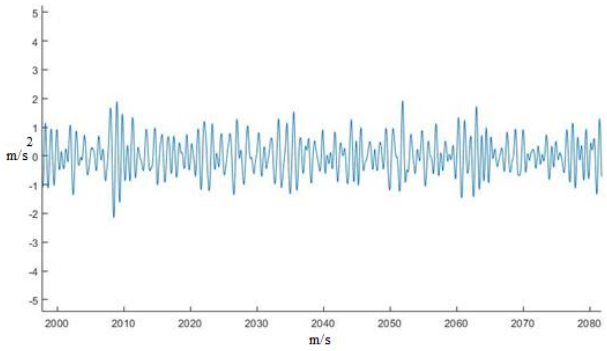

Fig 4. The implementation of acceleration. Normal bearing

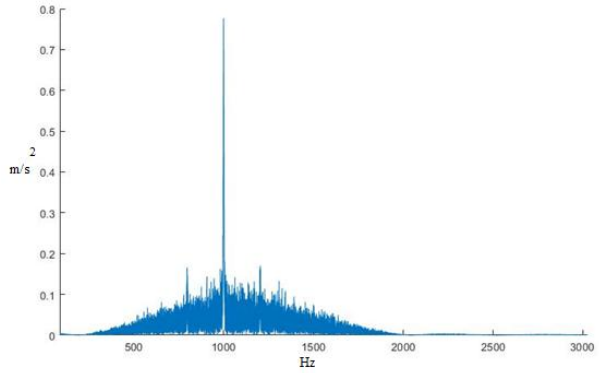

Fig. 5. Acceleration spectrum. Normal bearing

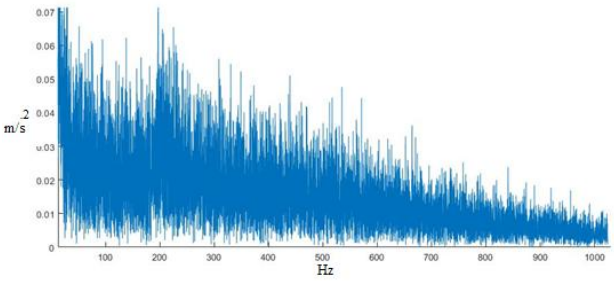

Fig. 6. Spectrum of the amplitude envelope of acceleration. Normal bearing

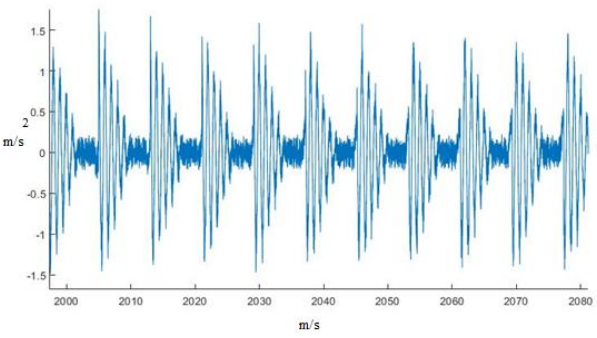

Fig. 7. Acceleration Implementation. Defective outer ring bearing

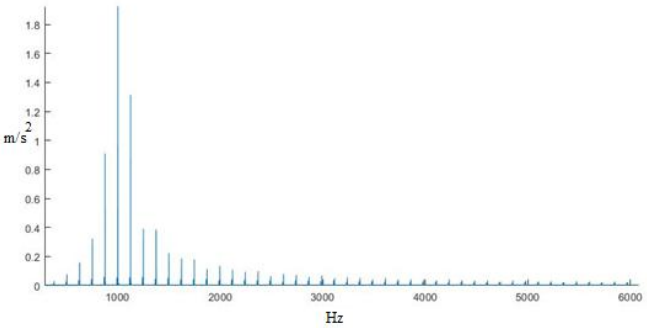

Fig. 8. Acceleration spectrum. Defective outer ring bearing

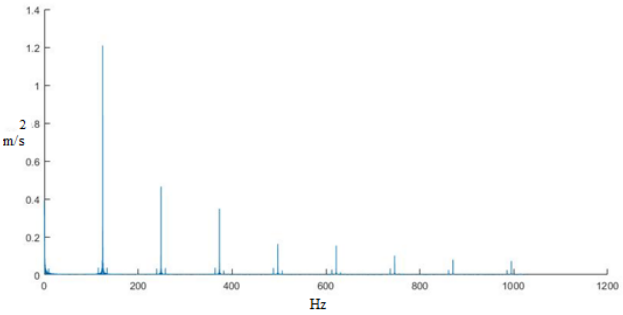

Fig. 9. Spectrum of the amplitude envelope of acceleration. Defective outer ring bearing.

To assess the adequacy of the model, vibration measurements were carried out on a 214 radial ball bearing, which was driven into rotation using a SP-180M drive unit. Overall dimensions of the bearing: outer diameter 125 mm, inner diameter 70 mm, width 24 mm, weight 1.08 kg. The measurements were carried out using the prototype of the specialized Vibro-ASIC microcircuit, and the AC-102 accelerometer was used as the primary transducer. In the tests, several bearings of the same type were used in different technical conditions: serviceable (no significant damage) and a bearing having a single damage on the outer ring. The measurements were carried out at a constant shaft rotation frequency of 30 Hz and an axial load of 440 N, the values of these parameters were selected in accordance with GOST 52545.2-2012. The force of pressing the vibration sensor to the outer ring of the bearing was 25 N. Industrial oil I-12 was used as a lubricant [23].

Consider the acceleration signal received on the LF channel in the band up to 10 kHz, Fig. 10, sample length 4096 samples (duration 80 ms), sampling frequency 25600 Hz. The spectrum obtained from the acceleration signal up to 10 kHz with a frequency resolution of 12.5 Hz is shown in Fig. 11. The spectrum of the amplitude envelope of the acceleration of the bearing up to 1000 Hz, with a frequency resolution of 1.25 Hz, is shown in Fig. 12.

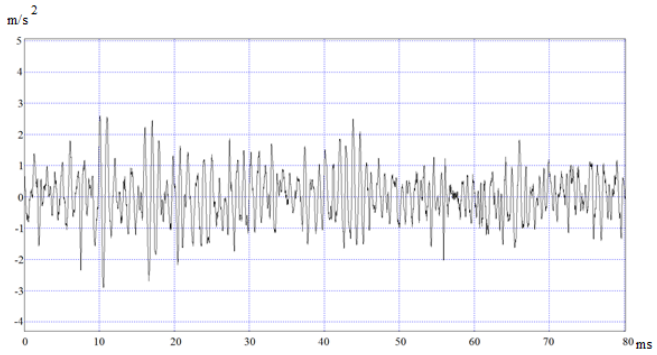

Fig. 10. The implementation of acceleration. Normal bearing.

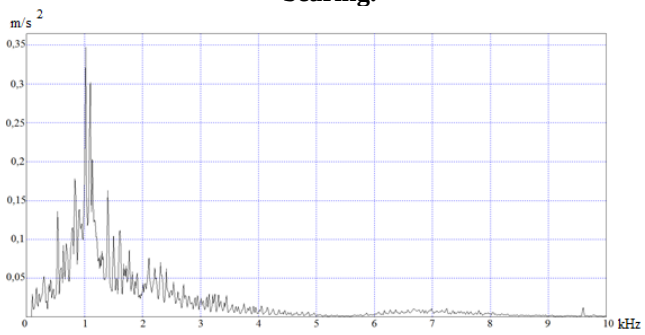

Fig. 11. Acceleration spectrum. Normal bearing

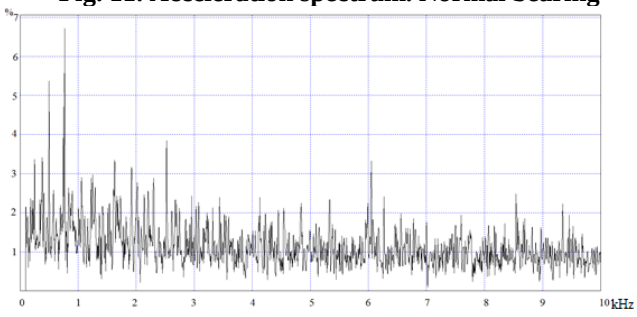

Fig. 12. Spectrum of the amplitude envelope of acceleration. Normal bearing.

Bearing vibration measurements with damage to the outer ring are presented below.

The measurement results are presented by the same measurements as a serviceable bearing, this is done so that the signals and spectra can be compared with each other [21, 22, 24].

The acceleration signal received on the LF channel in the band up to 10 kHz is shown in Fig. 13. The spectrum of accelerations up to 10 kHz is shown in Fig. 14. The spectrum of the amplitude envelope of the acceleration of the bearing is shown in Fig. 15.

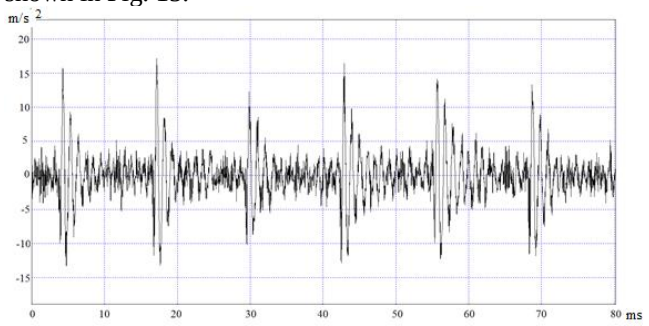

Figure 13. The implementation of acceleration. Defective outer ring bearing.

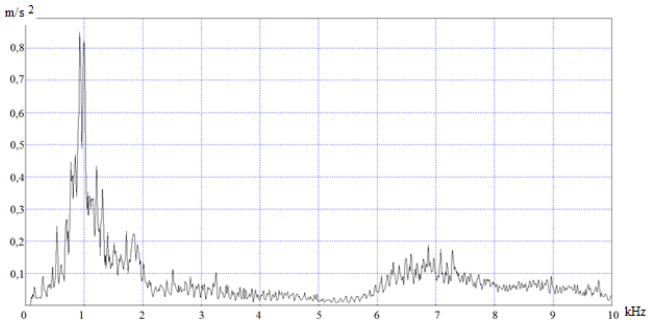

Fig. 14 Acceleration spectrum. Defective outer ring bearing.

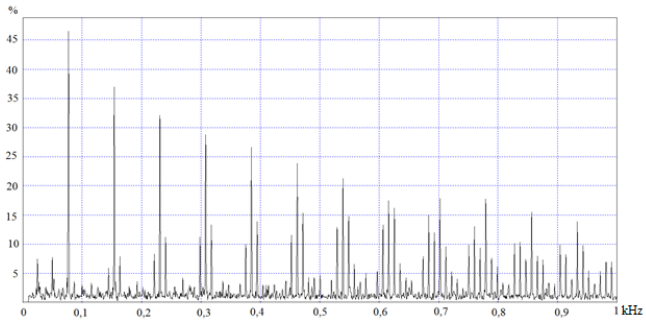

Fig. 15 Spectrum of the amplitude envelope of acceleration. Defective outer ring bearing.

IV. DISCUSSION

From a comparison of the waveforms, it can be seen that in the presence of defects in the bearing, the shape of the acceleration signal changes significantly, the differences can be easily differentiated. To automate the analysis of acceleration signals, it is more convenient to work not with the original acceleration signals, but to use spectral analysis of the envelope. The test shows that the Vibro-ASIC microcircuit makes it possible to differentiate different states of a rolling bearing according to acceleration signals, amplitude acceleration envelope and spectra of amplitude acceleration envelope.

V. CONCLUSION

The work shows a promising approach to machine learning of the vibrodiagnostic system, which consists in modeling the profile of kinematic disturbances in the time domain. The application of this approach will reduce the computational cost of hardware in the process of training a real system of vibration diagnostics. The adequacy of the proposed method is confirmed by calculations in Matlab and comparison with experimental data.

This work shows the possibility of sufficiently accurate reproduction of the vibrational characteristics of the bearing assembly with relatively low computational costs. This allows you to generate a large amount of training data for defect-free bearings, as well as for bearings with single and multiple defects.

ACKNOWLEDGMENT

The given work was made on support of the Ministry of Education and Science of Russian Federation on the Agreement about the providing of the subsidies №14.581.21.0030 from the 23th of October 2017, the unique identification of the work (project) is RFMEFI58117X0030.

REFERENCES

1. P.B. Gerike. "Monitoring the technical condition of drilling rigs of the DML series by parameters of mechanical vibrations", Vestnik nauchnogo tsentra po bezopasnosti rabot v ugol'noj promyshlennosti, 1, 2014p. 28-31.
2. V.I. Pisarev, A.A. Vaganov, A.F. Denisenko, and I.O. Tyuterev. "Maintenance and repair the metalworking tools with CNC of the basis of CIP diagnostics of the technical condition", Izvestija Samarskogo nauchnogo tsentra Rossijskoj akademii nauk, 16(1-2), 2014, pp. 508-513.
3. S.V. Rozhkov, G.V. Shadskiy, and V.G. Shadskiy. "Use of neural network apparatus to analyze vibration characteristics spindle assemblies for machine tools", Izvestija Tul'skogo gosudarstvennogo universiteta. Tekhnicheskije nauki, 8(2), 2017, pp. 271-275.
4. S. V. Korobkova. "Problems of efficient approximation of multidimensional functions using neural networks", Izvestija Yuzhnogo federal'nogo universiteta. Tekhnicheskije nauki, 58(3), 2006, pp. 121-127.
5. M.B. Rahmoune, A. Hafaifa, and M. Guemana. "Fault Diagnosis in Gas Turbine Based on Neural Networks: Vibrations Speed Application", in Applied condition monitoring, 5, T. Fakhfakh, F. Chaari, M. Abdennadher, M. Abbes, and M. Haddar (Eds.). Cham: Springer International Publishing Switzerland, 2017, pp 1-11. DOI: 10.1007/978-3-319-41459-1_1
6. Z. Chen, X. Chen, C. Li, R.V. Sanchez, and H. Qin. "Vibration-based gearbox fault diagnosis using deep neural networks", Journal of Vibroengineering, 19(4), 2017, pp 2475-2496. DOI: 10.21595/jve.2016.17267
7. P. Chopra. "Making Your Neural Network Say "I don't know" - Bayesian NNs using Pyro and PyTorch", Towards Data Science, 2018. Retrieved from: https://towardsdatascience.com/making-your-neural-network-say-i-dont-know-bayesian-nns-using-pyro-and-pytorch-b1c24e6ab8cd (access date: 12.10.2019).
8. E.S. Gasparov. Providing dynamic quality of high-speed spindle units based on modeling and in-place assessment of the condition of the supports. PhD thesis Abstract, Samara, 2016. 173 p.
9. E.S. Gasparov. "Spindle assembly support model on rolling bearings," Vestnik Samarskogo gosudarstvennogo tekhnicheskogo universiteta. Tekhnicheskije nauki, 4(40), 2013, p. 98-105.
10. V.F. Zhuravlev, V.B. Balmont. Gyroscope Ball Bearing Mechanics. Moscow: Mashinostrojenije, 1986. 272 p.
11. A.-E.Yu. Witkut. "Transfer function between the geometry of manufacturing precision ball bearings and a variable moment of resistance", Vibrotekhnika, 3(8), 1969, pp. 85-90.
12. M.K. Leontiev. "Nonlinear models of rolling bearings in rotor dynamics", Vestnik Moskovskogo aviatsionnogo instituta, 19(2), 2012, pp. 134-145.
13. M.K. Leontiev, V.A. Karasev, O.Yu. Potapova, and S.A. Degtyarev. "The dynamics of the rotor in rolling bearings", Vibraysija mashin: izmerenije, snizhenije, zashchita, 4(7), 2006, pp. 40-45.
14. A.S. Kelson, Yu.N. Zhuravlev, and N.V. Yanvarev. Calculation and design of rotary machines. Leningrad: Mashinostroenije, 1977. 288 p.
15. M.A. Galakhov, A.N. Burmistrov. Calculation of bearing units. Moscow: Mashinostroenije, 1988. 336 p.
16. R.D. Beiselman. Rolling bearings: Ref. 6th ed. Moscow: Mashinostroenije, 1975. 574 p.
17. O.V. Cheremisina, T.E. Litvinova, and D.S Lutskiy. "Separation of samarium, europium and erbium by oleic acisolution at stoichiometric rate of extractant", *Innovation-Based Development of the Mineral Resources Sector: Challenges and Prospects, 11th conference of the Russian-German Raw Materials*, 2018, pp. 413-419.
18. D. Lutskiy, T. Litvinova, I. Oleijnik, and I. Fialkovskiy. "Effect of anion composition on the extraction of cerium (Iii) and yttrium (Iii) by oleic acid", *ARPN Journal of Engineering and Applied Sciences*, 13(9), 2018, pp. 3152-3161.
19. N.V. Dzhevaga, and O.L. Lobacheva. "Separation of the rare-earth elements (REE) by flotation approaches", *The International Multidisciplinary Scientific GeoConference Surveying Geology and Mining Ecology Management,SGEM 2018*, 18(5.1), 2018, pp. 801-808.
20. O. Lobacheva, and N. Dzhevaga. "Rare earth elements recovery on the exampleof europium (III) from lean technogenic raw materials", *Journal of Ecological Engineering*, 18(6), 2017, pp. 122-126.
21. O.L. Lobacheva, I.V. Berlinskii, and N.V. Dzhevaga. "Thermodynamics of complexation in an aqueous solution of Tb(lll) nitrate at 298 K", *Russian Journal of Physical Chemistry A*, 91(1),2017, pp. 67-69.
22. D.A. Ilyukhin, S.A. Ivanik, and A.S. Pevnev. Justification of method of continuous measurements of position of sides of surface mine. *IOP Conf. Series: Journal of Physics: Conf. Series 1118 (2018) 012017*. DOI: 10.1088/1742-6596/1118/1/012017
23. N.P. Senchina, E. Ermolin, and O. Ingerov. "Integration of ground audio-magnetotelluric (AMT) and airborne magnetic surveys for exploration of gold-bearing quartz veins", *GEOBAIKAL 2014 - 3rd International Geobaikal Conference 2014: Exploration and Field Development in East Siberia*.
24. R.K. Nadirov, L.I. Syzdykova, and A.K. Zhussupova. "Electrochemical recovery of gold from concentrate by using sulfur-graphite electrode as the leaching agent source", *Journal of Chemical Technology and Metallurgy*, 53(3), 2018, pp. 556-563
25. O.F. Putikov, and N.P. Senchina. "Precise Solution of the System of Nonlinear Differential Equations in Partial Derivatives of the Theory of Geoelectrochemical Methods", *Doklady Akademii Nauk (Doklady Earth Sciences)*, 2(463), 2015, pp. 726-727.
26. K.R. Nadirov, L.I. Syzdykova, and A.K. Zhussupova, "Copper smelter slag treatment by ammonia solution: leaching process optimization", *Journal of Central South University*, 24, 2017, pp. 2799-2804.